

Seismic performance of three-storey full-scale sub-standard reinforced concrete buildings

Mustafa Comert¹ · Cem Demir¹ · Ali Osman Ates¹ ·
Kutay Orakcal² · Alper Ilki¹

Received: 8 May 2016 / Accepted: 25 September 2016
© Springer Science+Business Media Dordrecht 2016

Abstract Two three-story full-scale sub-standard reinforced concrete buildings were tested under self-weight and reversed cyclic lateral displacements to examine their behavior during earthquakes. While one of these buildings was a part of an actual existing building (TB1) built in the beginning of 1990's in Istanbul, the other was constructed by the authors as a representative building (TB2) that reflects the most common structural deficiencies of existing building stock in Turkey. Both buildings were constructed with plain bars, low strength concrete and inadequate lateral reinforcement. The differences between these buildings were axial load levels of first story columns, expected location of major structural damages (weak beam–strong column for TB1 and strong beam–weak column for TB2) and connection details of longitudinal bars in columns at the foundation–column interface (continuous for TB1 and lap-spliced with 180° hooks for TB2). Both buildings were pushed and pulled at increasing displacement amplitudes up to near collapse well beyond the life safety performance level. While TB1 was damaged significantly at 1.5 % inter-story drift ratio, TB2 reached near collapse damage at 4.0 % inter-story drift ratio. In this paper, details and test results of these two sub-standard buildings are presented. In addition, the available nonlinear modeling techniques and performance predictions of the Turkish Seismic Design Code (Specification for the buildings to be

✉ Mustafa Comert
mcomert@itu.edu.tr

Cem Demir
demirce@itu.edu.tr

Ali Osman Ates
aliates@itu.edu.tr

Kutay Orakcal
kutay.orakcal@boun.edu.tr

Alper Ilki
ailki@itu.edu.tr

¹ Faculty of Civil Engineering, Istanbul Technical University, 34469 Maslak, Istanbul, Turkey

² Civil Engineering Department, Bogazici University, 34342 Bebek, Istanbul, Turkey

constructed in disaster areas. Ministry of Public Works and Settlement, Ankara, 2007), ASCE 41-13 (Seismic rehabilitation of existing buildings, ASCE/SEI 41-13. ASCE, Reston, 2014) and Eurocode 8-3 (Eurocode 8: Design of structures for earthquake resistance. Part 3: Assessment and retrofitting of buildings. Comité Européen de Normalisation, Bruxelles, 2005) are compared with the experimental results.

Keywords Building test · Field test · Column · Full scale · Lap-splice · Performance assessment · Reinforced concrete · Seismic behavior

1 Introduction

A major part of earthquake-prone settlement areas in the world comprise sub-standard building stock. These sub-standard buildings, which are typically constructed with poor reinforcement details and low strength concrete, generally suffer from destructive earthquakes, due to their low deformation capacity as well as insufficient lateral stiffness and strength. Moreover, these buildings incorporate various typical deficiencies such as corrosion of reinforcing bars, lack of concrete cover, inadequate reinforcement anchorage conditions and lack of maintenance. In addition to the fact that they generally do not meet the requirements prescribed in modern seismic codes, they also do not fulfill the design requirements at their time of construction. Consequently, in order to prevent potential loss of life and economic losses, and maintain a sustainable development of the built environment, seismic safety attributes of these buildings need to be urgently evaluated using proper methods to categorize whether or not they possess risk of life safety or collapse during severe earthquakes.

Reliability of available seismic safety assessment methodologies depends on the modeling and analysis approach followed, and the criteria used in defining acceptable damage levels. In earthquake performance assessment, the algorithms used for structural analysis and the assumed damage limits depend mainly on post-earthquake observations and results of laboratory tests. However, among various other uncertainties, post-earthquake investigations do not provide sufficient information on the earthquake demand parameters on the building, such as internal force and deformation demands on the structural members, unless the building is densely instrumented for structural health monitoring purposes. In the case of laboratory tests, the physical and financial constraints deter the researchers from performing full-scale tests that can more realistically mimic the seismic behavior of actual structures. With field testing of real structures; boundary conditions, uncertainties and randomness in material characteristics and construction practice are more realistically considered. In this context, field tests carried out on real-life structures may emerge as a reasonable alternative for creation of benchmark data for verification of the available structural analysis approaches and assessment methodologies. Perhaps, the field testing of real structures also has its own challenges such as; less control for the variables, difficulties in supplying adequate excitation force capacity, establishment of strong reaction walls, need for large number of sensors and data collection systems, high dependence on weather conditions, need for a devoted team, and the cost for establishment and running of the test site.

Although there exist a limited number of laboratory tests on full/large scale reinforced concrete (RC) buildings, including pseudo-dynamic (Negro et al. 2004, 2013; Balsamo

et al. 2005; Di Ludovico et al. 2008; Bournas et al. 2013), shaking table (e.g., Garcia et al. 2010, 2014; Quintana-Gallo et al. 2010) and quasi-static (Pujol and Fick 2010) tests, very few field testing studies on existing buildings (Della Corte et al. 2006; Hwang et al. 2008; Kabeyasawa et al. 2012; Hsiao et al. 2015) have been conducted previously by researchers. This study aims to generate benchmark full-scale test data for sub-standard buildings with deficiencies including low concrete quality, plain bars, light transverse reinforcement and inadequate reinforcement details.

This paper presents test results of two full-scale RC buildings (Test Building 1 and Test Building 2) subjected to reversed cyclic lateral loading. Both buildings reflect the main characteristics and deficiencies of existing sub-standard buildings in Turkey as well as various other developing countries. Test Building 1 (TB1) is part of an existing building more than 20 years old, which was demolished partially to obtain the test structure. It should be noted that partial demolishing was executed very carefully, not to impose any damage on the remaining part of the building to be tested. Test Building 2 (TB2) was designed by the authors to also reflect typical characteristics of existing sub-standard buildings, and was constructed at the same site. Although both buildings are representative of the same vulnerable building stock, they differ from each other in specific aspects including axial load levels on the columns, reinforcement details, and the expected hierarchy of damage developing on the beams and columns. In addition to visual observations on the evolution of damage, the behavior of the buildings is characterized by using the load–displacement data collected at the story levels and the deformation measurements at the potential plastic hinging regions of the beams and columns. Finally, predictions of the seismic performance assessment approaches recommended by ASCE 41-13 (2014), Turkish Seismic Design Code (TSDC 2007) and Eurocode 8-3 (2005) are compared with the test results and observations.

2 Fikirtepe test area

The experimental phase of the study, which includes reversed cyclic loading tests on two full-scale buildings, was implemented at the Fikirtepe district of Istanbul city. The area is home to hundreds of sub-standard buildings, which lack appropriate engineering design, construction practice, and supervision. Based on the Urban Transformation Law (Law No. 6306 on the Transformation of Areas Under Disaster Risk), that aims to reconstruct or retrofit seismically vulnerable buildings on a mass scale, the area has recently been designated as a high seismic risk area and was abandoned for demolition at the time of testing. Considering a number of factors including the availability of area for construction of the reaction wall and the second test building, availability of the test site during the entire period of the testing project, compatibility of the test building with characteristics of the existing building stock, accessibility to site, access to power and water, and the technical capabilities of the available test equipment; the reinforced concrete building shown in Fig. 1 was selected for execution of the test program. The existing three-story building was standing at the bottom of a steep slope, so that the entrance to the original building was from the third story. In order not to exceed the limitations of the load capacities of the reaction wall, as well as the hydraulic actuators and the load cells used, the existing building was demolished partially so that the remaining part was designated as Test Building 1 (TB1) (as shown in Fig. 1), and the site was arranged for construction of the reaction wall and Test Building 2 (TB2), as shown in Fig. 2a. After partial demolishing of



Fig. 1 General view of the test site and plan of the existing building



Fig. 2 a Layout of the test site and b–d stages of site preparation

the existing building, the test site was leveled and lean concrete was poured, which was followed by construction of a 0.6 m thick mat foundation (Fig. 2b). The mat foundation not only supported the reaction wall and TB2, but also TB1, which only had unreinforced footings with approximately 0.15 m thickness underneath the columns. In the next step,

construction of the 0.5 m thick reaction wall took place, which was followed by construction of the second test building (Fig. 2c, d). The 7.0 m high reaction wall had an oblique W-shaped cross-section in plan, so that it provided the sufficient stiffness and lateral load capacity for the two buildings to be tested consecutively, only by repositioning of the hydraulic actuators (Fig. 2a).

3 Properties of the test buildings

During the experimental phase of the study, the two full-scale buildings with reinforced concrete moment resisting frames were tested under reversed cyclic lateral loads. Both three-story buildings incorporated bare frames without infill walls, and had one span in each orthogonal x and y directions. Typical plan views of Test Building 1 (TB1), which was extracted from the existing building, and Test Building 2 (TB2), which was designed and constructed by the authors, can be seen in Fig. 3.

TB1, which was constructed during the first half of 1990s, had 2.7 m story height on all three stories. The plan dimensions measured from exterior surfaces of the beams were approximately 3.5 m by 4.1 m. The beams in x-direction of the building extended for an additional length of 0.6 m from the column surfaces in order to supply adequate anchorage length on the beam longitudinal bars, since the adjacent bay of the building was demolished. Non-structural elements such as hollow clay brick infill walls and plaster covering on beam and column surfaces were removed for preventing potential interference with the structural system. Before and after the partial demolition phase, the building was surveyed for measuring of dimensions and investigation of material characteristics and reinforcement layout. Concrete cores (100 mm × 200 mm cylindrical cores) were sampled from each story and were tested under uniaxial compression, which indicated an average concrete compressive strength of 17 MPa. The general workmanship quality was low, so that the alignment of the reinforcing bars before concrete pouring, formation of the concrete cover around the reinforcement and compaction of concrete was problematic. Reinforcement of the structural members consisted of plain bars, which was typical for the time of construction. Uniaxial tension tests carried out on steel samples obtained from the demolished sections of the building provided average yield strength values of 290 and 370 MPa for the longitudinal and transverse bars, respectively. The beams had 150 mm × 500 mm cross-sectional dimensions, with two 10 mm and one 12 mm diameter longitudinal bars at the top and two 12 mm diameter bars at the bottom of the support cross-sections. Three of the four columns at each of the first and second stories of TB1 had cross-sectional dimensions of 250 mm × 500 mm, whereas the fourth column (S14) had 300 mm × 650 mm cross-section. All columns had six 16 mm bars as longitudinal reinforcement. In the third story of the building, all columns had approximately 250 mm × 400 mm cross-sectional dimensions and incorporated six 16 mm longitudinal bars, except one column that had four 16 mm bars (S31 column). The column longitudinal bars in the first story of the building were continuous down to the foundation, instead of being spliced above the foundation level, probably because the building did not have a proper foundation system. The transverse reinforcement of beams and columns comprised 8 mm diameter stirrups tied at an approximate spacing of 300 mm, with absence of confinement regions at potential plastic hinge locations. As commonly observed in sub-standard buildings, the hooks of the closed stirrups were bent at 90°.

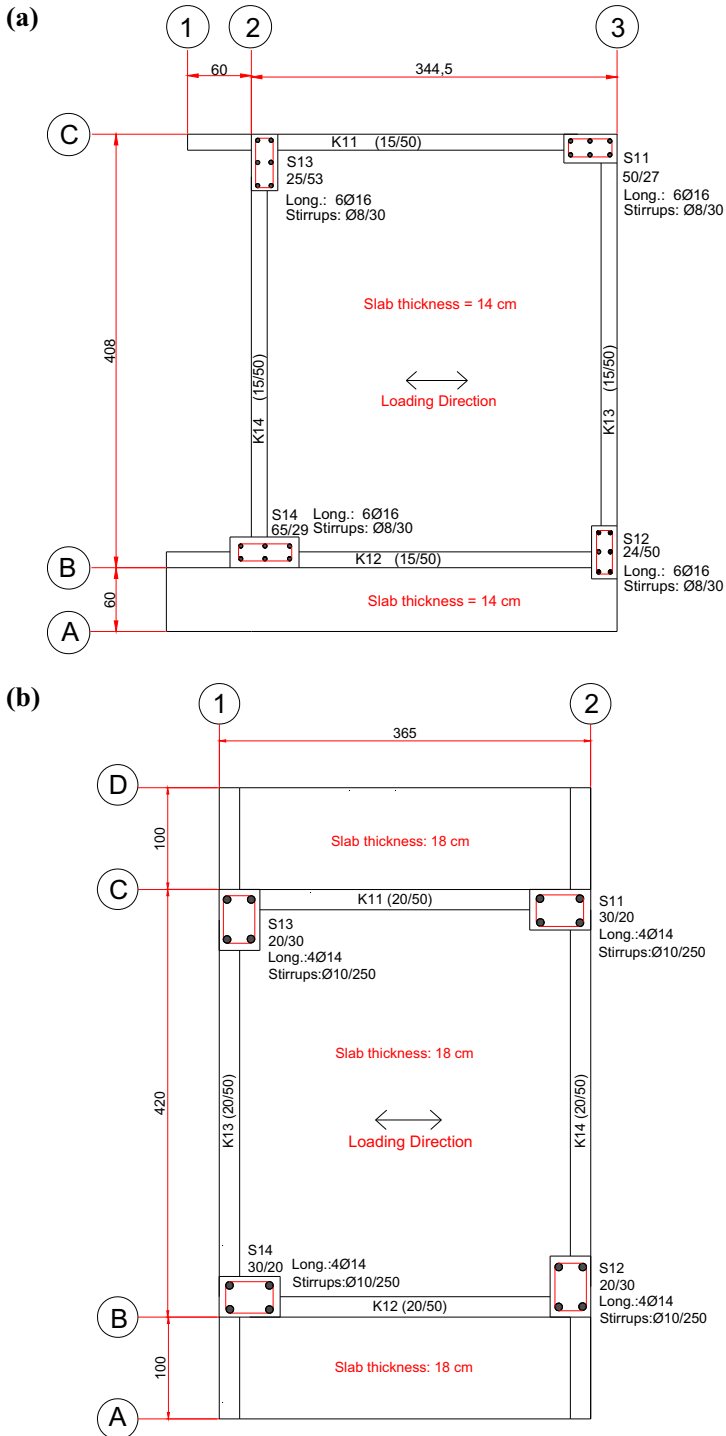


Fig. 3 Plan and reinforcement layouts of **a** TB1 and **b** TB2 at 1st story

TB2, which was designed and constructed to also represent existing sub-standard buildings in Turkey, had dimensions of 4.20 m \times 3.65 m in plan. The 0.18 m thick slab and beams with 200 mm \times 500 mm cross-sections were elongated as 1 m long overhangs on both sides of the building, for increasing the axial load levels of the columns. Each story of the three-story moment resisting frame structure with 1 \times 1 spans in x and y directions was 3 m high. All columns had cross-sectional dimensions of 200 mm \times 300 mm and were reinforced using four 14 mm longitudinal bars and 10 mm stirrups with 250 mm spacing and 90° hooks. The beams had cross-sectional dimensions of 200 mm \times 500 mm, with five 12 mm diameter longitudinal bars at the top and four 12 mm diameter bars at the bottom of the support cross-sections. The beam transverse reinforcement was identical to columns, and no special confinement regions were provided on either beams or columns. The concrete mix used during the construction of TB2 was designed to intentionally obtain low strength concrete, so that an average compressive strength of 10 MPa was achieved (based on results of tests on 150 mm \times 300 mm cylinders) on the 28th day after pouring. The ready-mixed concrete was produced at a concrete plant and was transported to the test site. The average yield strength of the plain longitudinal and transverse reinforcing bars was obtained from uniaxial tension tests as 350 MPa. Lap splice length for column longitudinal reinforcement was 75 times the diameter of the longitudinal bars (75ϕ) at the first story (above the foundation level), whereas a lap splice length of 50ϕ (above the story level) was used in construction of the second and the third story columns. 180° hooks were formed at the ends of both starter and longitudinal bars in the lap splice regions.

Although both TB1 and TB2 were representative of existing sub-standard buildings, they differentiated from each other in certain aspects including column axial load ratios, connection details of longitudinal bars at story levels, flexural yielding hierarchy at beam-column joints, observed construction qualities (relatively better for TB2), and relatively lower strength concrete used for TB2. The average axial load acting on the first story columns of TB1 (at the absence of lateral loads) was approximately 6–10 % of the column axial load capacities calculated considering only the contribution of concrete (6 % for S14, 7 % for S11 and S13 and 10 % for S12), whereas the same ratio was approximately 23 % for first story columns of TB2. Regarding moment capacity ratios of columns and beams at beam-column joints, building TB1 had the favorable strong column–weak beam configuration, since the columns theoretically had greater bending moment capacities compared to the beam support sections. However, TB2 was intentionally designed and constructed to exhibit a more common mechanism observed in existing sub-standard buildings after major earthquakes; namely, the weak column–strong beam configuration. For this purpose, the theoretical (calculated) bending moment capacities of the first story columns of TB2 were designed to be 65 % of that of the beam support cross-sections.

4 Test setup

Both buildings TB1 and TB2 were subjected to quasi-static reversed cyclic lateral loading. For this purpose, three servo-controlled hydraulic actuators with 300 kN load and 800 mm displacement capacities were mounted on the reaction wall and attached to the buildings at first and second story (floor) levels, as shown in Fig. 4. Attachment of the actuators to each floor was accomplished by bolting the plate of the actuator swivel-head to one of two steel plates located at both extremities of the building, which are connected together using post-tensioned threaded steel rods that run above and below the reinforced concrete slab and

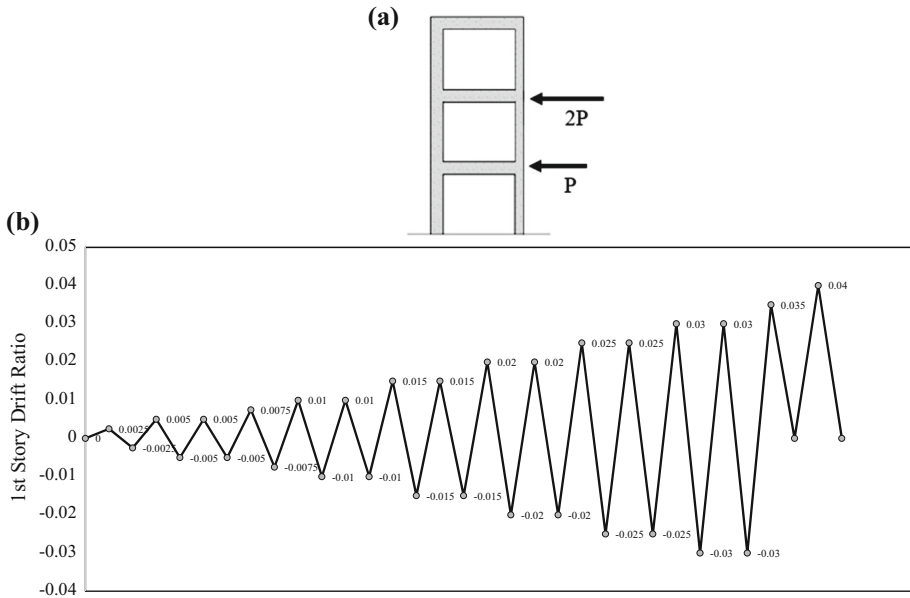


Fig. 4 **a** Loading setup and **b** loading protocol

pass through holes drilled on beams spanning in the transverse direction of loading. This demountable connection system was chosen since the accompanying dynamic identification tests presented in a companion paper (Goksu et al. 2015) were performed at different damage levels and required removal of the hydraulic actuators from the building. Rather than using one actuator at each story level, two actuators were attached to the second story of the test buildings so that any possible torsional effects could be countered.

The gravitational loads acting on the columns of the test buildings were supplied by the self-weights of the buildings themselves. In the case of TB1, no additional vertical loads for live loads (quasi-permanent loads) were applied, since the 200 kg/m^2 live load value recommended by the Turkish Standards (TSE 1997) for live loads acting on the slabs of residential buildings, merely corresponded to 0.1 % of axial load capacity of the first story columns. Similarly, no additional vertical loads were applied to TB2 which was designed and constructed with 18 cm thick reinforced concrete slabs that also accounted for the live loads, so that, higher axial load ratios could be achieved for the columns of this building.

The tests were conducted under displacement control, except for the initial loading cycles of TB2, which were performed partially under force control due to malfunctioning of one of the actuator displacement transducers. Throughout testing, the ratio of lateral loads acting on the second and first stories were kept equal to two, so that the first free vibration mode shape of the buildings were conformably followed, as also specified in nonlinear performance assessment procedures. The displacement cycles were applied considering specific drift ratio levels. Target drift ratios were defined for the critical first story of the buildings and included one or two loading cycles at following drift ratios: 0.25, 0.5 % (two cycles), 0.75, 1.0 % (two cycles), 1.5 % (two cycles), 2.0 % (two cycles), 2.5 % (two cycles) and 3.0 % (two cycles). In the case of TB1, for safety reasons, the test was terminated upon unloading from a drift ratio of 1.5 %, due to development of extensive damage on the building including buckling of column longitudinal

reinforcement. During testing of TB2, extensive measures were taken against potential total collapse by placing strong steel piers below the first floor level of the building. Consequently, reversed cyclic loading was applied on TB2 up to a drift ratio of 3.0 %, after which the building was pushed in one direction to drift ratios of 3.5 and 4.0 % under one-cycle repeated-cyclic loading.

The measurement system, which collected data from approximately 80 channels, consisted of data loggers, load cells, displacement transducers and strain gauges. General layout of the measurement system can be seen in Fig. 5. The first and second story-level lateral displacements were measured by the internal displacement transducers of the actuators as well as external Linear Variable Differential Transformers (LVDTs) mounted on stiff reference piers constructed using steel profiles. The lateral loads applied on the structure were monitored using the internal load cells on the actuators. Deformations at potential plastic hinging regions of the beams and columns were measured using longitudinal displacement transducers with a measurement (gauge) length of $h/2$, where h is the depth of the beam or column cross-section. Additional displacement sensors were also used at the bottom of the first story columns, where internal forces and deformations were

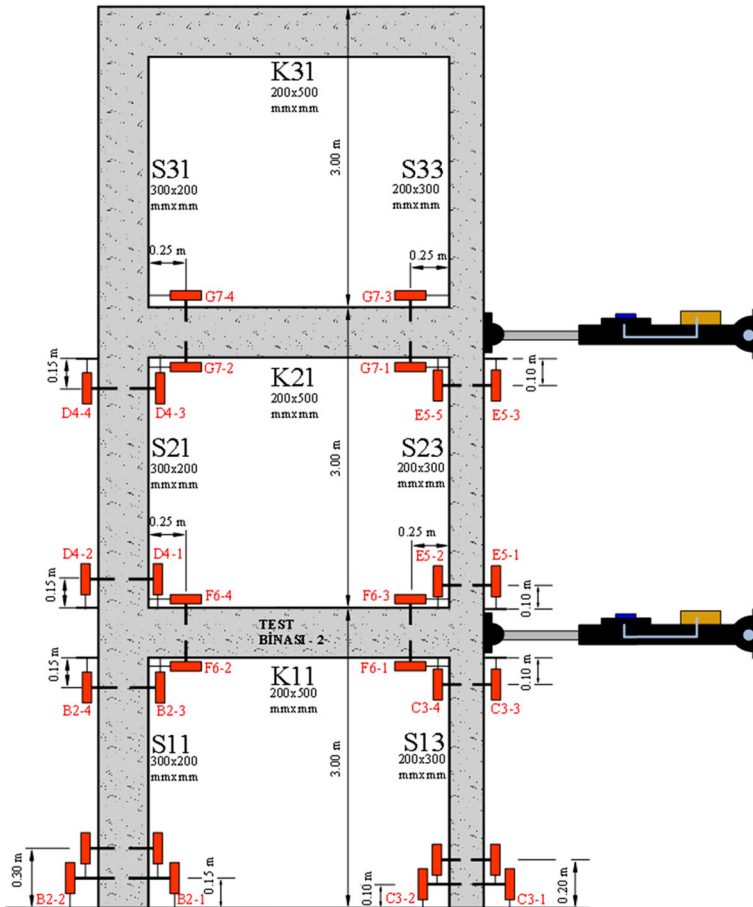


Fig. 5 Instrumentation layout

expected to be higher. These additional transducers spanned a gauge length equal to the depth of the column cross-section. In case of TB2, strain gauges were also bonded on the longitudinal reinforcement of the first-story columns.

5 Tests results

5.1 Results for TB1

The reversed cyclic loading pattern was imposed on the building up to a drift ratio of 1.50 %. Since the damage level attained at this drift ratio was substantial, the test was terminated at this drift level for safety reasons. It should be noted that, in the following results, the load values recorded while pushing the building are referred as positive loads, while the pulling loads are denoted as negative loads. The base shear vs. 1st story drift ratio response of TB1 is provided in Fig. 6. Marks on this figure indicate important stages of the test. Throughout the test, as also predicted during pre-test analyses, no significant shear damage was observed on the building (mainly due to the significant contribution of concrete to shear capacity that was higher than the experienced shear forces) and the overall response was governed by nonlinear flexural behavior at the critical end regions of beams and columns. The damage was first observed at the support regions of the first-story beams parallel to the loading direction (K11 and K12 in Fig. 3). Afterwards, damage started to accumulate at the bottom end regions of the first-story columns S11 and S14 (Fig. 7), which were stiffer and stronger in the loading direction than columns S12 and S13. During the following loading cycles, the level of damage on the beams intensified more rapidly than the columns. Since the thickness of concrete cover on the beams was only about 5 mm, concrete spalling occurred at an early stage at the beam end regions. The bottom longitudinal bars of beam K12 started to buckle during the loading cycles to 0.75 % drift

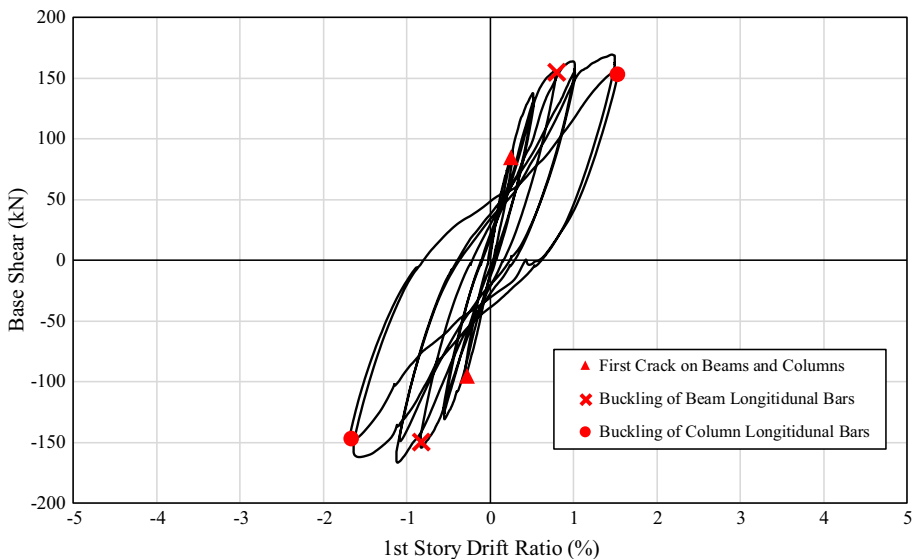


Fig. 6 Base shear—1st story drift ratio response of TB1

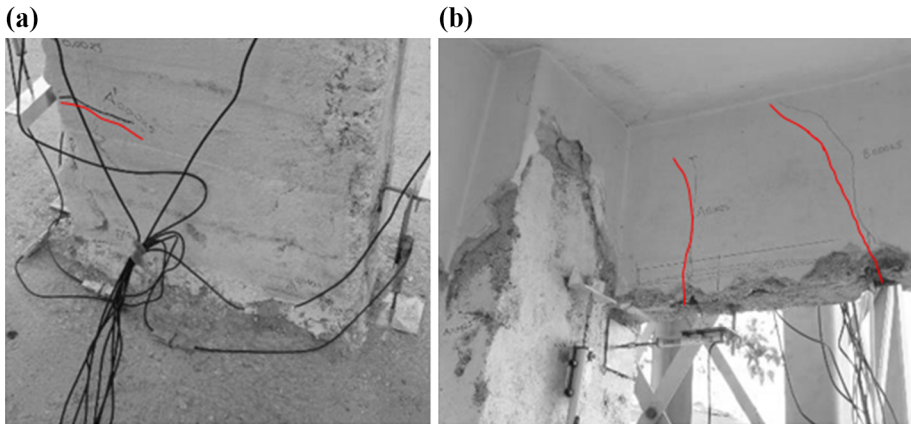


Fig. 7 First cracks observed **a** S14 column and **b** K11 beam at 0.25 % drift ratio

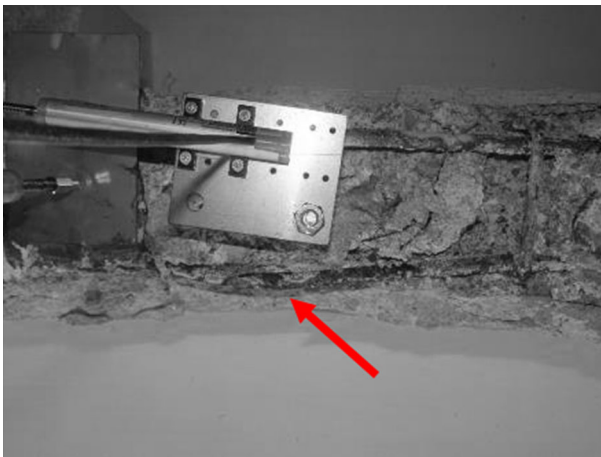


Fig. 8 Buckling of longitudinal bars of beam K12 at 0.75 % drift ratio

(Fig. 8). When a drift ratio of 1.0 % was reached, almost all bottom longitudinal bars at the end regions of the first-story beams, that were parallel to the loading direction, had buckled. Following buckling of beam longitudinal bars, the bottom end regions of the first-story columns started to experience extensive damage. Vertical cracks and cover crushing were observed on column S14 at 1.0 % drift ratio (Fig. 9), and the longitudinal bars of column S14 buckled at 1.5 % drift ratio (Fig. 10). No significant damage was observed on columns S12 and S13 of the first story, which were weaker in the loading direction. As well, no significant damage (apart from flexural cracking) was observed in any of the beams or columns located in the second or third stories of the building. Average longitudinal strains along a length of $0.5h$ at the column base (where h is the depth of the column cross-section) were measured using two transducers installed on the opposite faces of the column in the direction of bending. Similarly, average longitudinal strains along the potential plastic hinging regions of the beams were measured using displacement transducers attached to the top and bottom of the beam end regions. Measurements of these

Fig. 9 Vertical crack on column S14 at 1.00 % drift ratio

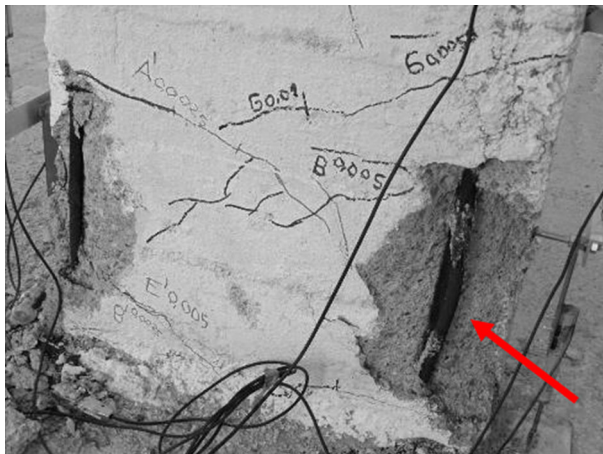


Fig. 10 Buckling of longitudinal bars of column S14 at 1.50 % drift ratio

transducers were used for calculation of beam and column end rotations. The measured longitudinal strain versus drift ratio and base shear versus end rotation response of severely shear damaged members (S14 and K12) are presented in Figs. 11 and 12. As can be seen in these figures, the maximum average tensile and compressive strain values measured on column S14 are recorded as 0.018 and 0.065, respectively. Additionally, the end rotations created by these longitudinal strains at the bottom of column S14 is 0.012 at a story drift ratio of

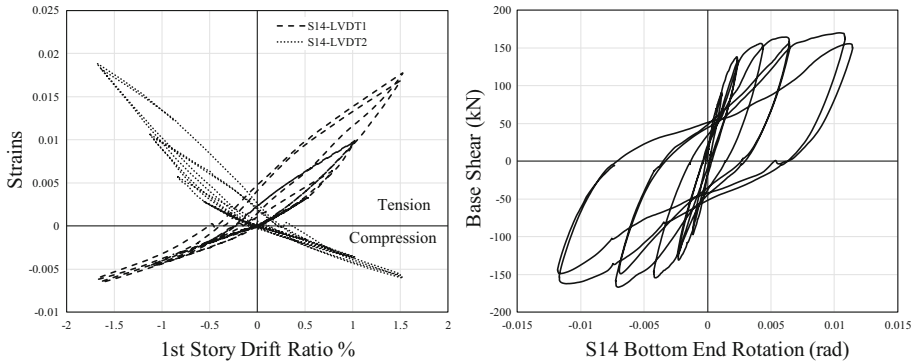


Fig. 11 Strain and end rotation measurements of column S14

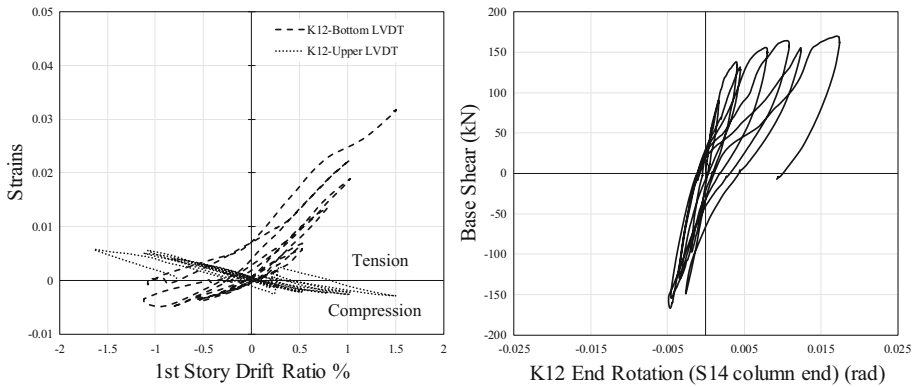


Fig. 12 Strain and end rotation measurements of K12 beam

1.5 %. The maximum tensile strains measured along the uppermost and lowermost longitudinal fibers at the support cross-section of beam K12 are 0.005 and 0.03, respectively. This difference can be attributed to the contribution of the slab to on the bending flexural behavior of the beam in under positive bending moment direction. The maximum compressive strains measured on the beam were approximately 0.004 along both the uppermost and lowermost fibers.

5.2 Results for TB2

The entire loading protocol shown in Fig. 4 was imposed on this building. The test was stopped at a drift ratio of 4.0 %, at which the building lost 40 % of its lateral load capacity. The measured base shear versus first-story drift ratio response is provided in Fig. 13. Since the beams of this building had higher bending moment capacities than the columns, damage was concentrated at the column end regions, and almost no damage (other than minor flexural cracking) was observed on the beams. All columns in the first story of the building failed due to flexural effects and no shear damage occurred despite the 250 mm stirrup spacing (again mainly due to the significant contribution of concrete to shear capacity). The first flexural cracks were observed at the upper and lower end regions of the

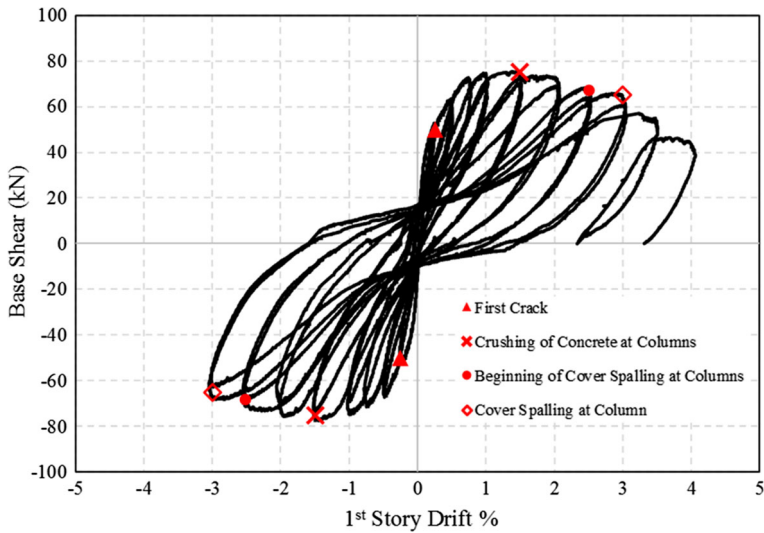


Fig. 13 Base shear—1st story drift ratio response of TB2

first-story columns at a drift ratio of 0.25 % (Fig. 14). First signs of concrete crushing were observed on column S11, at a drift ratio of about 1.5 % (Fig. 15). Cover spalling was observed on columns S11 and S13 at approximately 2.5 % drift ratio (Fig. 16). Average longitudinal strains measured using the displacement transducers installed along the potential plastic hinging regions of the columns and beams were used for calculation of the member end rotations. Additionally, strain gauges were affixed to the starter bars at the bottom of the first story columns of TB2. The distances between the foundation level and

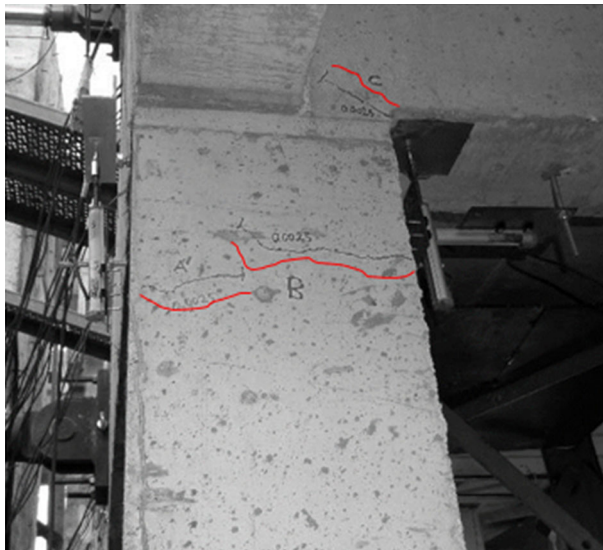


Fig. 14 First cracks observed at 0.25 % drift ratio on column S14

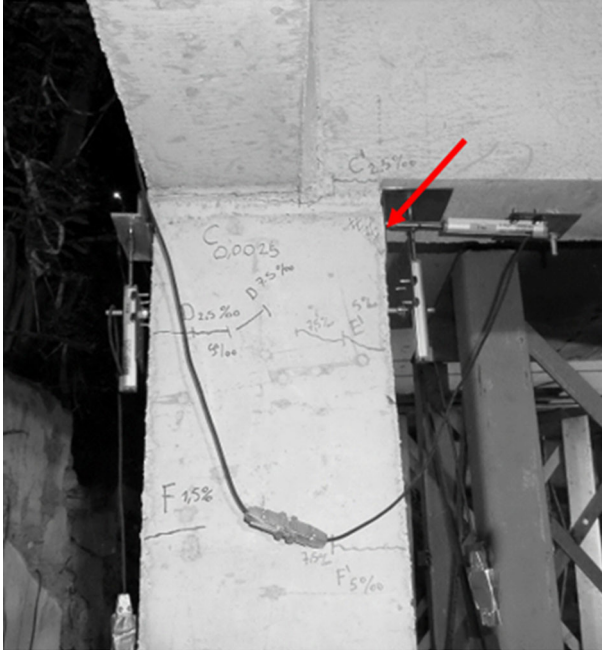


Fig. 15 Cover crushing at 1.50 % drift ratio in column S11



Fig. 16 Cover spalling at 2.50 % drift ratio in column S11

the location of these strain gauges were $0.25h$, $0.5h$, $0.75h$, and h (where h is the column depth in the direction of loading). The measured longitudinal strain versus drift ratio and base shear versus end rotation curves for column S11 are presented in Fig. 17a and b. Accordingly, while the maximum average tensile strains recorded by the transducers were approximately 0.065, the maximum strains measured by the strain gauges only reached about 0.0043 (15 times less than transducer measurements). As seen in Fig. 17c, the end rotations calculated using the measurements of the longitudinal transducers on column S11 were approximately 0.04 at first-story drift ratio of 4.00 %.

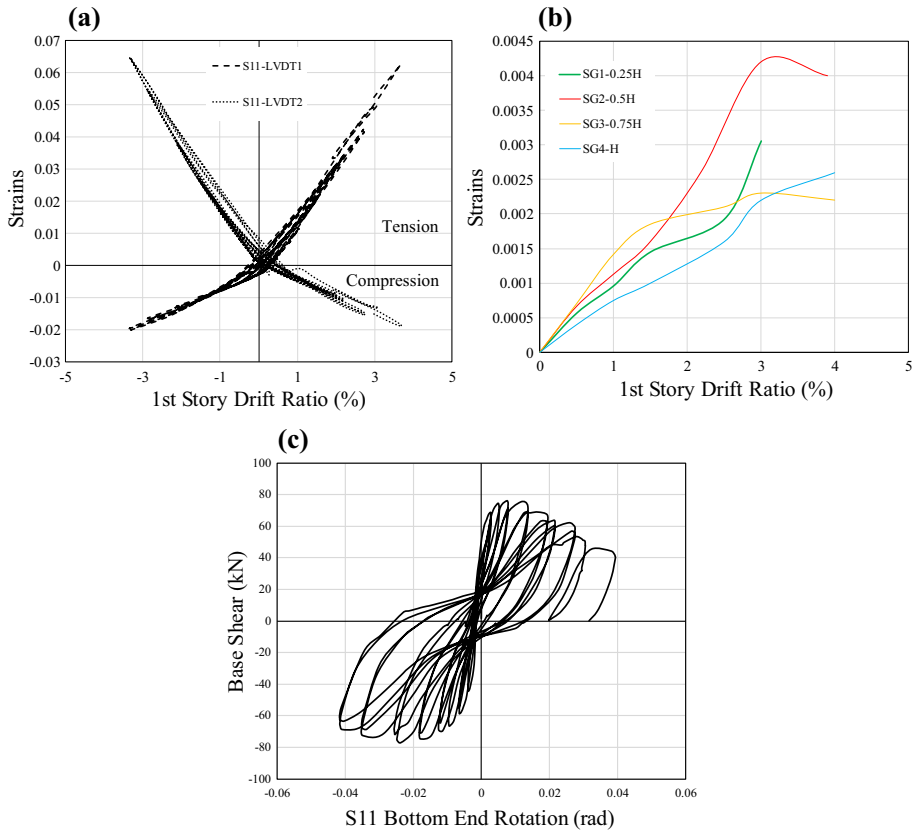


Fig. 17 **a** Average strains measured by LVDTs, **b** local strains measured by strain gauges and **c** end rotation measurements of column S11

5.3 Discussion of test results

Although they incorporated similar structural deficiencies (i.e. low strength concrete, plain bars and inadequate transverse reinforcement), observations made during the tests point to quite different types of structural behavior and performance for buildings TB1 and TB2. While TB1 was heavily damaged at a drift ratio of 1.5 % (cover spalling and longitudinal bar buckling in columns and beams), TB2 was in the range of moderate to heavy damage at a drift ratio of 4.0 % (no significant concrete spalling and no reinforcement buckling). Moreover, although the column end rotations recorded at similar drift ratios of TB2 were greater than TB1, the level of damage observed on the columns of TB2 was less than that of TB1. The reason for these contradictions might be sought in the differences of the test buildings. The tested buildings differentiated from each other with respect to their column axial load levels ($0.06\text{--}0.1f_c b h$ for TB1 and $0.23f_c b h$ for TB2), moment capacity hierarchy at beam-column joints (weak beam–strong column for TB1 and strong beam–weak column for TB2), use of different anchorage details on the longitudinal bars of the first story columns (continuous in TB1—type I anchorage, and 75ϕ lap-splices with hooks in TB2—type II anchorage, as seen in Fig. 18), observed construction quality (relatively better for TB2), and relatively higher deformability of low strength concrete used for TB2. At first

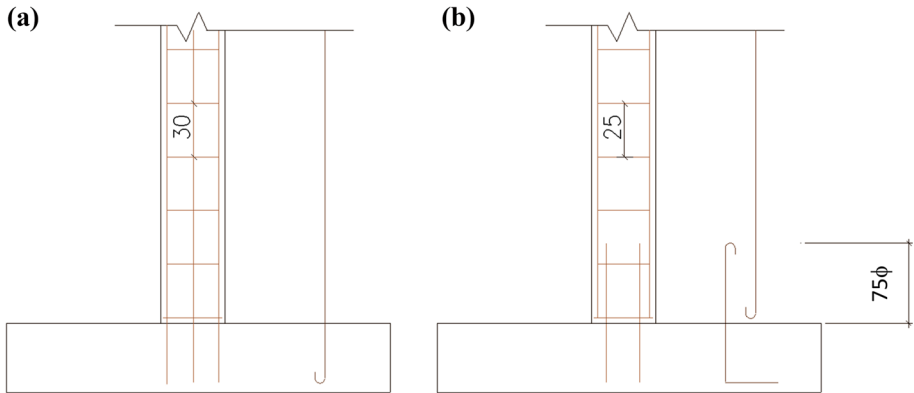


Fig. 18 Column longitudinal bar anchorage detail **a** type I (continuous) and **b** type II (lap-spliced)

glance, it may be expected that the lower axial load levels of the columns and the strong column–weak beam configuration would affect the structural behavior positively in terms of deformation capacity and evolution of the damage. Possible reasons that can help to explain the discrepancy in the observed structural responses of TB1 and TB2 in means of damage progress, are the difference in column longitudinal bar anchorage details, lower quality of workmanship observed at TB1 and relatively lower strength of concrete used for TB2. As also mentioned previously, the low workmanship quality of TB1 resulted with inadequate and irregular concrete cover thickness and random concrete quality distribution that eased the spalling of concrete and premature buckling of the longitudinal bars. Additionally, TB2 was constructed by using a lower strength concrete, which is known to be more deformable than medium strength concrete.

In the type II anchorage detail used in construction of the columns in TB2, the starter and longitudinal bars at the lap splice incorporate 180° hooks at the ends. As also indicated by Fabbrocino et al. (2004), during seismic actions, these hooks behave like semi-rigid ends with very limited slip, while the straight region of the bar loses its bond to concrete at strain and stress levels much lower than yield. Due to debonding along the straight region, the starter bars deform uniformly along the entire lap-splice length, and under same story displacement (and column end rotation) levels, this phenomenon causes smaller average tensile strains in the reinforcing bars (and therefore smaller average compressive strains in concrete) compared to the continuous type I anchorage condition. When this happens, visual inspection of the damage on the column indicates formation and progressive widening of a single flexural crack at the column–foundation interface, and the column exhibits a rocking-like behavior. This was also observed on the first story columns of building TB2 (with type II anchorage detail). While the damage observed on column S14 of TB1 was distributed along an approximate height of 300 mm from the column base (approximately $0.5h$, where h is the depth of the column cross-section) as shown in Fig. 10, the flexural deformation observed at the base of column S11 in TB2 was localized along the first few centimeters of the column (due to formation of a distinct interface crack), as can be seen in Fig. 19. The strain gauge measurements done for S11 column also gives hint about this behavior. Accordingly, the local tensile strains measured along the longitudinal bar (at 0.25, 0.50, 0.75 and 1.0 H distance from the column bottom) point to close values to each other (i.e. strains vary between 0.0013 and 0.0023 at 2 % drift ratio), as seen in

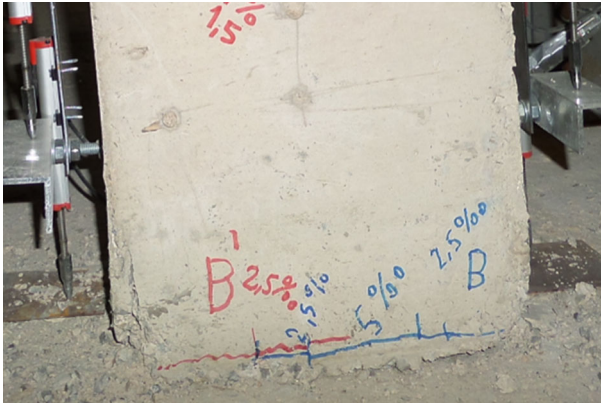


Fig. 19 Distinct single crack observed on column S11

Fig. 17b. The similar behavior was also seen on cantilever column tests with type II anchorage details conducted by Goksu et al. (2014).

6 Performance predictions of available nonlinear assessment approaches

The test buildings were modeled and analyzed using code-compliant nonlinear analysis approaches and the performance of the analysis procedures and member damage limits specified in Turkish Seismic Design Code (TSDC 2007), ASCE 41-13 (2014) and Eurocode 8-3 (2005) were evaluated. A widely used and commercially available software (Perform 3D, 2011) was utilized for the structural analyses, in which material and geometric nonlinearities were both considered. Material nonlinearity was incorporated following the well-known lumped plasticity approach, in which rotational plastic hinges are assigned to the potential plastic hinging regions of the columns and beams. For evaluating the response prediction capability of the pushover analysis method defined in TSDC (2007) and Eurocode 8-3 (2005), the nonlinear flexural behavior of columns and beams were obtained from section analyses (in means of moment–curvature relationships). During section analyses, the constitutive material models for concrete and reinforcement were considered as suggested in the documents. In addition, plastic hinge length (L_p) are assumed to be $L_p = 0.5H$ (H is the flexural depth of cross section) for evaluation of TSDC (2007) and $L_p = 0.2H(1 + (1/3)\min(9; L_s/H))$ for Eurocode 8-3 (2005), where L_s is the shear span of the members. In this study, the plastic hinge length equation used for Eurocode 8-3 (2005) is taken from Fédération Internationale du Béton (FIB) (2012), since a valid plastic hinge length equation for columns with smooth bars is not proposed in Eurocode 8-3 (2005). While assessing the accuracy of the Nonlinear Static Procedure defined in ASCE 41-13 (2014), the plastic hinge properties of columns and beams were both defined by utilizing the backbone curves specified in ASCE 41-13 (2014). Single-mode pushover analyses were conducted in the loading direction of each test building. The distribution of lateral loads applied at story levels during the analyses, were compatible with the tests; P at first story level, $2P$ at second story level and zero load at third story level. In addition to modeling and analysis criteria, both performance assessment documents define limits for predicting member damage (or performance) levels. The member damage (performance) limits defined in the evaluated documents are indicated in Table 1. The TSDC

Table 1 The member damage (performance) limits defined in the documents

TSDC (2007)	Minimum damage (MN)	Safety limit (SL)	Collapse limit (CL)
ASCE 41-13 (2014)	Immediate occupancy (IO)	Life safety (LS)	Collapse prevention (CP)
Eurocode 8-3 (2005)	Damage limitation (DL)	Significant damage (SD)	Near collapse (NC)

(2007) method defines the damage levels in terms of strains in concrete and longitudinal reinforcement under flexural behavior, whereas, the ASCE 41-13 (2014) and Eurocode 8-3 (2005) use plastic rotations and chord rotation in defining damage (performance) limits, respectively. In this study, for achieving compatibility between the two procedures, the strain limits defined in TSDC (2007) are converted into equivalent plastic rotation limits at member ends, using results of strain compatibility (cross-sectional) analysis.

6.1 Prediction of member damage states

The experimental base shear versus member end rotation responses that were obtained for the first-story column S14 and beam K12 of TB1 and the first story-column S11 of TB2 are

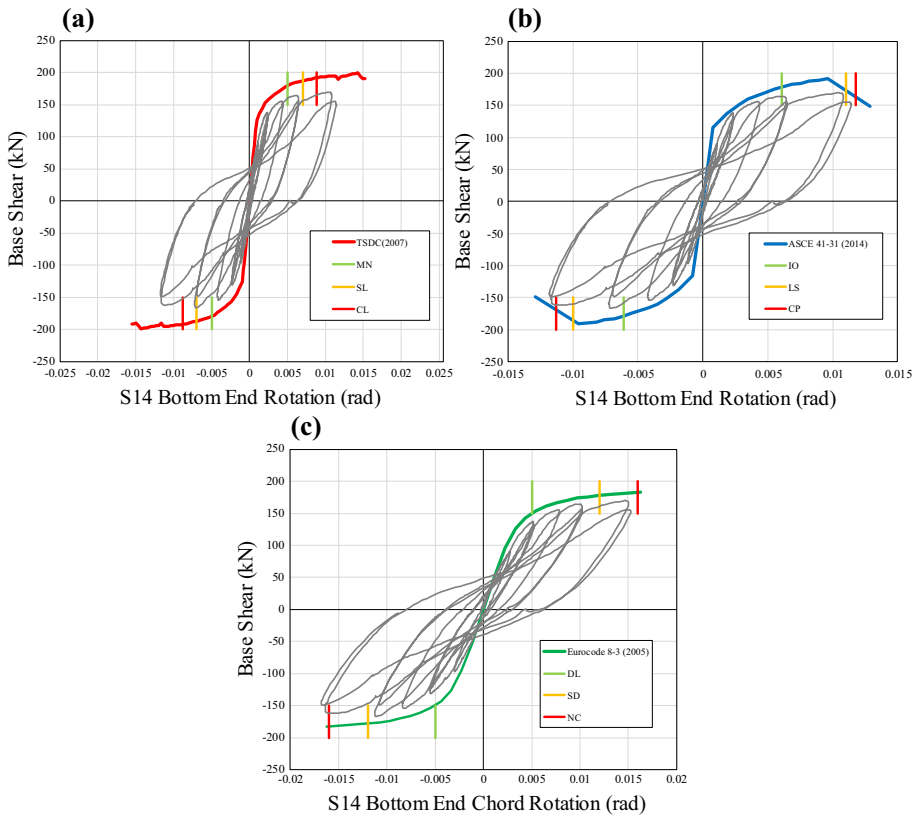


Fig. 20 Comparison of base shear versus end rotation curves for column S14 of TB1 **a** TSDC (2007), **b** ASCE 41 (2014) and **c** Eurocode 8-3 (2005)

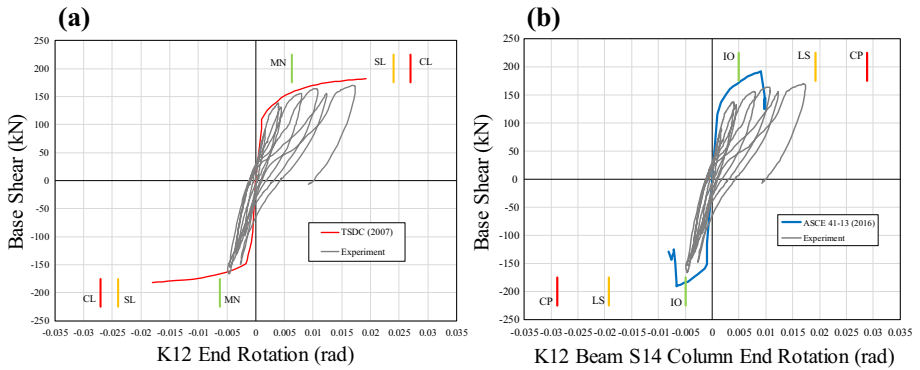


Fig. 21 Comparison of base shear versus end rotation curves for beam K12 of TB1 **a** TSDC (2007) and **b** ASCE 41 (2014)

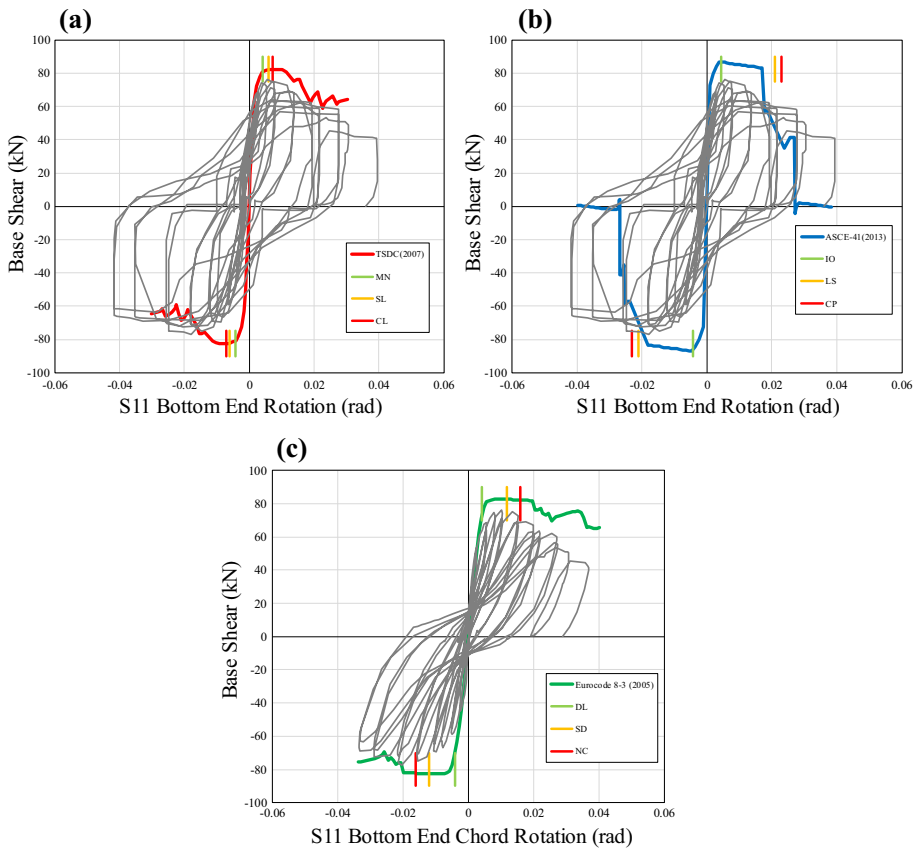
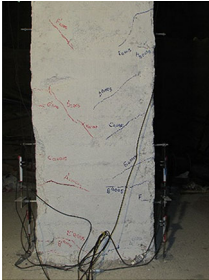

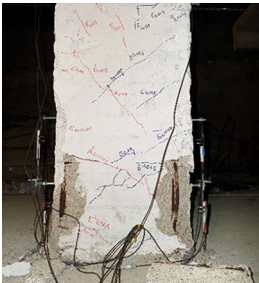


Fig. 22 Comparison of base shear versus end rotation curves for column S11 of TB2 **a** TSDC (2007), **b** ASCE 41 (2014) and **c** Eurocode 8-3 (2005)


compared with the theoretical responses obtained from the two performance assessment procedures in Figs. 20, 21 and 22. The member damage limits defined in the TSDC (2007), ASCE 41-13 (2014) and Eurocode 8-3 (2005) documents are also shown in these figures (the comparison of experimental results of K12 beam with Eurocode 8-3 (2005) are not given since the experimental chord rotation of this member cannot be calculated from available measurements). Furthermore, the damage limits and the observed damage at corresponding rotation levels for column S14 and beam K12 of TB1, as well as column S11 of TB2, are summarized in Tables 2, 3 and 4, respectively. For column S14 of TB1, as can be seen in Fig. 20 and Table 2, although the ASCE 41-13 (2014) and Eurocode 8-3 (2005) defines approximately 20–30 % larger rotation limits compared to the TSDC (2007), all analysis procedures and damage limitations are in overall good correlation with

Table 2 Comparison of member damage predictions with test results for column S14 of TB1

	TSDC (2007) ^a (rotation)	ASCE 41-13 (2014) (rotation)	Eurocode 8-3 (2005) (chord rotation)	Observed damage	Damage notes
MN, IO, DL	0.005	0.0061	0.005		(As observed at 0.75 % drift ratio) Distributed flexural cracks were observed. Maximum residual crack width is measured as 0.5 mm
SL, LS, SD	0.0071	0.011	0.012		(As observed at 1.00 % drift ratio) Concrete spalling. Maximum residual crack width is measured as 1.1 mm
CL, CP, NC	0.009	0.012	0.016		(As observed at 1.25–1.50 % drift ratio) Buckling of longitudinal bars

^a TSDC (2007) defines damage limits in terms of material strains. The corresponding rotations are calculated using sectional analysis

Table 3 Comparison of member damage predictions with test results for beam K12 of TB1

	TSDC (2007) ^a (rotation)	ASCE 41-13 (2014) (rotation)	Eurocode 8-3 (2005) (chord rotation)	Observed damage	Damage explanation
MN, IO, DL	0.006	0.005	0.006		(As observed at 0.75 % drift ratio) Buckling of longitudinal bars under compression
SL, LS, SD	0.024	0.019	0.019	Experimental rotation did not reach this level	–
CL, CP, NC	0.028	0.029	0.025	Experimental rotation did not reach this level	–







^a TSDC (2007) defines damage limits in terms of material strains. The corresponding rotations are calculated using sectional analysis

the test data and observations. The rotation limits that define the member damage states in TSDC (2007) seem to be slightly more conservative than those specified in other documents, when compared with each other and with the experimental observations presented in Table 2. For beam K12 of TB1, all procedures fail to estimate the observed level of damage (Fig. 21; Table 3). The damage observed on this beam during the test progressed much more rapidly than predictions. For beams of TB1, the diameter of the beam longitudinal bars (d) is 12 mm and the spacing of stirrups (s) is approximately 300 mm. Together with the thin concrete cover, the s/d ratio that is in the order of 25 makes the beam longitudinal bars prone to buckling (as also observed during testing of TB1). In predicting the beam damage state, all assessment approaches lack the consideration of beam compression bar buckling, which leads to misprediction of the behavior, ductility, and damage state of the beam.

For the first story column S11 of TB2, performance assessment results and experimental observations are compared in Table 4 and Fig. 22. It is evident that for this column, ASCE 41-13 (2014) defines much larger rotation limits when compared to TSDC (2007) and Eurocode 8-3 (2005). This difference can be attributed to the dependency of the damage limits to the volumetric ratio of transverse reinforcement in the ASCE 41-13 (2014). On the other hand, the TSDC (2007) method does not consider the amount of existing transverse reinforcement as a parameter in defining the damage limit, unless the transverse reinforcement is properly detailed. Since the requirements for properly detailed transverse reinforcement are stringent (e.g., 135° hooks on column ties, with adequate hook length), most columns of sub-standard buildings are classified in the TSDC (2007) approach as unconfined, and conservative values for damage limits are obtained. However, in ASCE 41-13 (2014), different conditions are defined for detailing of transverse reinforcement (e.g., 90° closed hoops). No information about details of transverse reinforcements is provided in Eurocode 8-3 (2005).

The level of damage observed on the first story column S11 of TB2 during the test is quite different than the predicted by the performance assessment procedures, as also shown in Table 4. Even at the high rotation limits specified in ASCE 41-13 (2014), the observed damage was limited to minor concrete cover spalling and small residual crack widths. This

Table 4 Comparison of member damage predictions with test results for column S11 of TB2

	TSDC (2007) ^a (rotation)	ASCE 41-13 (2014) (rotation)	Eurocode 8-3 (2005) (chord rotation)	Observed damage 0.005 rotation					
MN, IO, DL	0.004	0.004	0.0041			Flexural cracks were observed. Maximum crack width is measured as 0.5 mm			
SL, LS, SD	0.006	0.021	0.012	0.0075 rotation	0.01 rotation	0.015 rotation			
							Flexural cracks were observed. Maximum crack width is measured as 1.0 mm		
							Flexural cracks were observed. Maximum crack width is measured as 1.5 mm		
MN, IO, DL	0.0072	0.023	0.016	0.02 rotation	0.025 rotation				
							Minor cover spalling. Flexural cracks were observed. Maximum crack width is measured as 3.0 mm		
							Minor cover spalling. Flexural cracks were observed. Maximum crack width is measured as 4 mm		

^a TSDC (2007) defines damage limits in terms of material strains. The corresponding rotations are calculated using sectional analysis

inconsistency can be attributed to the experimentally observed rocking behavior of the columns in TB2, due to loss of bond and slippage of longitudinal bars. This observation is a clear indication of the effect of the reinforcement detailing (e.g., using column splices with 180° hooks) at critical regions of structural members on the response, which can significantly alter the overall behavior or failure mode of existing buildings during earthquakes. The modeling approaches available in the TSDC (2007) and ASCE 41-13 (2014)

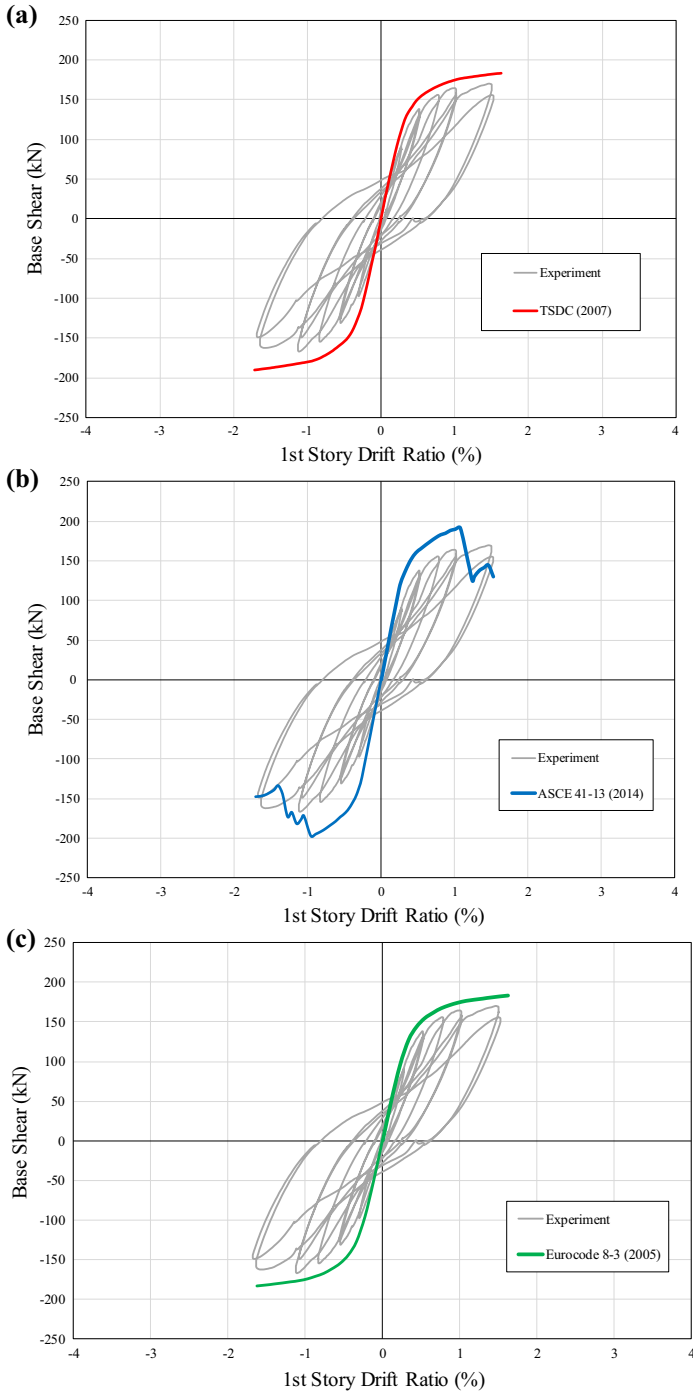


Fig. 23 Comparison of test results and analysis results for TB1 **a** TSDC (2007), **b** ASCE 41 (2014) and **c** Eurocode 8-3 (2005)

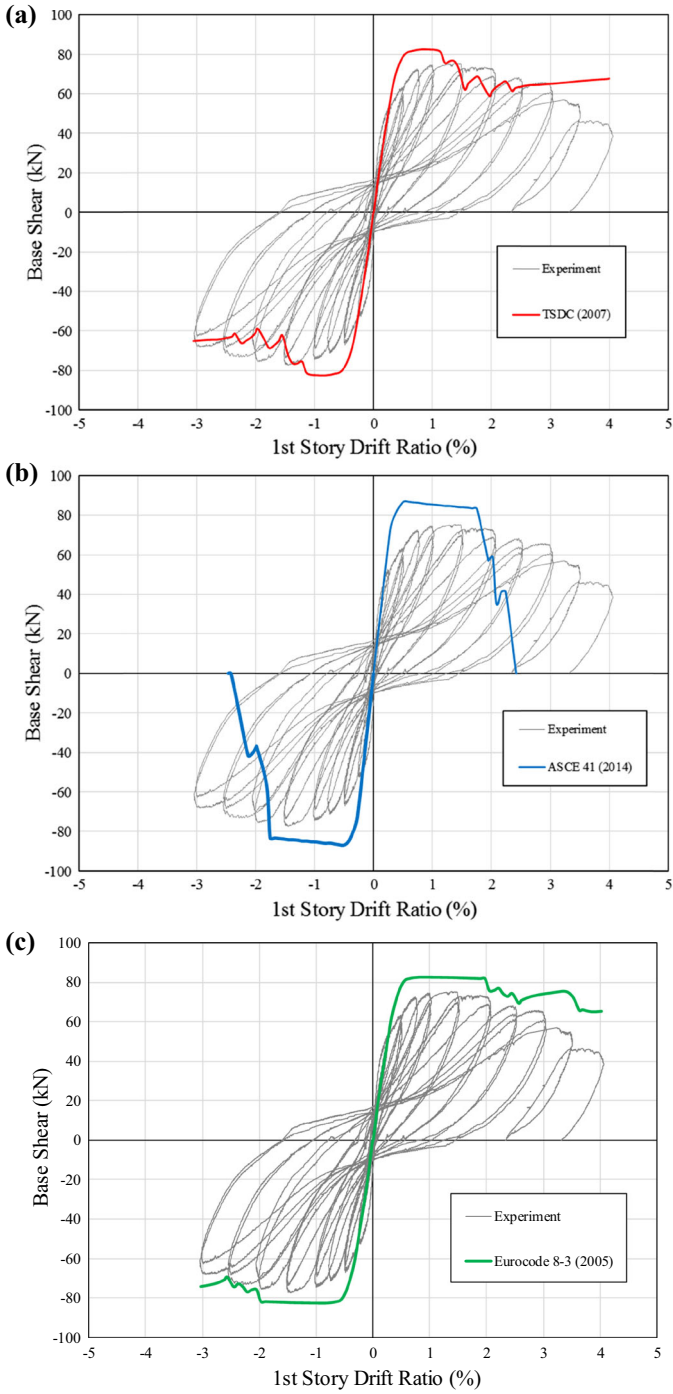


Fig. 24 Comparison of test results and analysis results for TB2 **a** TSDC (2007), **b** ASCE 41 (2014) and **c** Eurocode 8-3 (2005)

documents do not provide suggestions for idealization of the behavior of this type of anchorage detail, and the associated behavioral characteristics cannot be effectively considered during the performance assessment procedure. The only document that considers the details of longitudinal bars is Eurocode 8-3 (2005). This document defines reduction factors to chord rotation limitations for members constructed with continuous plain bars (like TB1) or plain bars with 180° hooks (like TB2). However, when the predictions are compared with the observed damages of the columns of TB2 (built with plain and 180° hooked bars), a conservatism still exists for prediction of damage states of members having this type of connections since the member rotations caused by slip of longitudinal bars and 180° hooks are not taken into account in modelling procedure and damage limits.

6.2 Pushover curve predictions

The predictions of all seismic performance assessment procedures for the base shear versus first-story lateral drift ratio response of both buildings are compared with the experimentally measured cyclic responses in Figs. 23 and 24. All modeling approaches well-predict the initial stiffness of the buildings, yet overestimate their lateral load capacity by approximately 10–20 %. Except over prediction of lateral strength, the pushover curves predicted for TB1 by the TSDC (2007), ASCE 41-13 (2014) and Eurocode 8-3 (2005) procedures show similar trend up to a drift ratio 1 %. After this point, while the ASCE 41-13 (2014) procedure predicts a sudden decrease in lateral load capacity, the TSDC (2007) and Eurocode 8-3 (2005) pushover curves do not estimate loss in lateral load up to the maximum drift ratio of 1.5 % applied during the test. This difference between the pushover curves is related to the different approaches used for modeling of columns in the performance assessment procedures. While the ASCE 41-13 (2014) backbone curves defined for plastic hinge rotations in columns incorporate a sudden decrease in the moment vs. plastic rotation behavior, the TSDC (2007) and Eurocode 8-3 (2005) did not estimate the strength loss up to larger deformations. In the case of TB2, the consideration of the plastic hinges, which was followed for the TSDC (2007) and Eurocode 8-3 (2005) approach, indicated a better agreement with the test results. Similar to TB1, the ASCE 41-13 (2014) pushover curve for TB2 exhibited a sudden drop in lateral load at a drift ratio of approximately 2 %. The experimentally observed flexural yielding hierarchy at the beam-column connections of both buildings was captured by all assessment procedures (beams of TB1 reached flexural capacity before columns and columns of TB2 reached flexural capacity before beams). However, it should be recalled that none of the performance assessment procedures accurately predicted the experimentally observed damage states of the structural members.

7 Conclusions

In this study, the behavior of two sub-standard buildings under gravity loads and lateral displacement reversals were investigated through full-scale field tests and performance evaluation procedures. Although both buildings were representative of the existing sub-standard building stock in Turkey, they differentiated from each other in terms of axial load levels on columns, strong column–weak beam conditions, and anchorage details of the column longitudinal bars.

The following results are drawn from the test observations and comparisons of test results with predictions of code-based seismic performance assessment procedures conducted on these buildings:

- The evolution of damage was highly affected by the moment capacity hierarchy between the beams and columns at the beam-column joints.
- In contrast with the estimations, the test building with the weak column–strong beam configuration and higher level of axial load on the columns (TB2) exhibited a more ductile behavior compared to building with a lower axial load level on the columns and a strong column–weak beam condition (TB1). The difference in the lateral displacement capacities and damage progress of the two test buildings is mainly attributed to the anchorage details of column longitudinal bars together with higher deformability of lower strength concrete used for TB2. In the case of lap-spliced longitudinal bars with 180° hooks at bar ends, debonding along the straight region of the lap splice influences the overall response of the building remarkably, causing larger rotations and leading to a pseudo-ductility.
- Comparison of experimental results and test observations with seismic performance predictions obtained using the Turkish Seismic Design Code (2007), ASCE 41-13 (2014) and Eurocode 8-3 (2005) procedures shows that all procedures may fail to predict the experimentally-observed behavior, particularly the damage (or performance) levels in the structural members and the rotation limits associated with these performance levels.
- In the case of columns of TB1, the prediction documents show better correlation with experimental results with respect to beams of TB1. For beams of this building, all documents fail to predict the damage accurately. The damage observed on the beams of this building during the test progressed much more rapidly than predictions (while the beam longitudinal bars in compression buckled at 0.75 % drift ratio, the documents allow more than 2 % drift ratio for collapse prevention damage state). The inclusion of longitudinal bars under compression with large s/d ratios while determining the damage limits, can cause unsafe overestimation of chord rotations corresponding to different performance limits.
- For TB2, TSDC (2007) and ASCE 41-13 (2014) lack suggestions for consideration plain round longitudinal bars with 180° hooks, which may significantly influence the overall structural behavior, as also observed during this test campaign. In the case of Eurocode 8-3 (2005), although the document applies reduction factors for chord rotation capacity of members with plain and 180°-hooked bars, the predictions still indicate too conservative results when compared with experiments.
- Full-scale testing of existing buildings may provide a good basis for evaluating the capabilities, limitations, and reliability of available modeling approaches and performance assessment procedures.

Acknowledgments Authors acknowledge the financial support provided by Istanbul Development Agency (Project No: TR10/12/AFT/0050), ITU Scientific Research Fund Department. The contributions of Erkan Tore, Ozgun Ozeren, Alvand Moshfeghi, Soheil Khoshkholghi, Caglar Goksu, Pinar Inci, Ugur Demir, Ahmet Sahin and 2014 summer trainees are also gratefully acknowledged. The authors are also thankful to supports of Akcansa Co., Art-Yol Co., Boler Celik Co., Hilti-Turkey Co., Tasyapi Co., Urtim Co., and Kadikoy Municipality.

References

- American Society of Civil Engineers (ASCE) (2014) Seismic rehabilitation of existing buildings, ASCE/SEI 41-13. ASCE, Reston, Virginia, USA
- Balsamo A, Colombo A, Manfredi G, Negro P, Prota A (2005) Seismic behavior of a full scale RC frame repaired using CFRP laminates. *Eng Struct* 27(2005):769–780
- Bournas DA, Negro P, Molina FJ (2013) Pseudodynamic tests on a full-scale 3-storey precast concrete building: behavior of the mechanical connections and floor diaphragms. *Eng Struct* 57(2013):609–627
- CEN (2005) Eurocode 8: Design of structures for earthquake resistance. Part 3: Assessment and retrofitting of buildings. Doc. CEN/TC250/SC8/N388B. Comité Européen de Normalisation, Bruxelles
- Computers and Structures Inc. (2011) 3D performance based design software. Perform 3D v5, California, USA
- Della Corte G, Barecchia E, Mazzolani FM (2006) Seismic Upgrading of RC buildings by FRP: full scale tests of a real structure. *J Mater Civ Eng* 18:659–669
- Di Ludovico M, Manfredi G, Mola E, Negro P, Prota A (2008) Seismic behavior of a full scale RC structure retrofitted using GFRP laminates. *J Struct Eng* 134:810–821
- Fabbrocino G, Verderame GM, Manfredi G, Cosenza E (2004) Structural models of critical regions in old-type rc frames with smooth rebars. *Eng Struct* 26(14):2137–2148
- Fédération Internationale du Béton (FIB) (2012) Model Code 2010—final draft, vol 1, Bulletin 65, and vol 2, Bulletin 66, Lausanne, Switzerland
- Garcia R, Hajirasouliha I, Pilakoutas K (2010) Seismic behavior of deficient RC frames strengthened with CFRP composites. *Eng Struct* 32(2010):3075–3085
- Garcia R, Hajirasouliha I, Guadagnini M, Helal Y, Jemaa Y, Pilakoutas K, Mongabure P, Chrysostomou C, Kyriakides N, Ilki A, Budescu M, Taranu N, Ciupala MA, Torres L, Saiidi M (2014) Full-scale shaking table tests on a substandard RC building repaired and strengthened with Post-Tensioned Metal Straps. *J Earthq Eng* 18(2):187–213
- Goksu C, Yilmaz H, Chowdhury SR, Orakcal K, Ilki A (2014) The effect of lap splice length on the cyclic lateral load behavior of RC members with low-strength concrete and plain bars. *Adv Struct Eng* 17(5):639–658
- Goksu C, Inci P, Demir U, Yazgan U, Ilki A (2015) Field testing of substandard RC buildings through forced vibration tests. *Bull Earthq Eng*. doi:[10.1007/s10518-015-9799-x](https://doi.org/10.1007/s10518-015-9799-x)
- Hsiao FP, Oktovianus Y, Ou YC, Luu CH, Hwang SJ (2015) A pushover seismic analysis and retrofitting method applied to low-rise RC school buildings. *Adv Struct Eng* 18(3):311–324
- Hwang SJ, Chiou TC, Hsiao FP, Chiou YJ, Alcocer SM (2008) Field test of RC school building retrofitted by post-tensioned rods. In: Proceedings of the fourteenth world conference on earthquake engineering, Beijing, China, 12–17 October 2008
- Kabeyasawa T, Kabeyasawa T, Hosokawa Y, Kim Y (2012) Static and dynamic loading test on base foundation in a reinforced concrete school building. In: Proceedings of the fifteenth world conference on earthquake engineering, Lisboa, Portugal, 24–28 September 2012
- Negro P, Mola E, Molina FJ, Magonette GE (2004) Full scale PSD testing of a torsionally unbalanced three-storey non-seismic RC frame In: Proceedings of the thirteenth world conference on earthquake engineering, Vancouver, Canada, 1–6 August 2004
- Negro P, Bournas DA, Molina FJ (2013) Pseudodynamic tests on a full-scale 3-storey precast concrete building: global response. *Eng Struct* 57(2013):594–608
- Pujol S, Fick D (2010) The test of a full-scale three-story RC structure with masonry infill walls. *Eng Struct* 32(2010):3112–3121
- Quintana-Gallo P, Pampanin S, Carr AJ (2010) Shake table tests of under-designed RC frames for the seismic retrofit of buildings-design and similitude requirements of the benchmark specimen. Paper presented at the 2010 NZSEE conference, Wellington, 26–28 March 2010
- Turkish Seismic Design Code (2007) Specification for the buildings to be constructed in disaster areas. Ministry of Public Works and Settlement, Ankara
- Turkish Standards Institute (TSE) (1997) Design loads for buildings, TS 498. Turkish Standards Institute (TSE), Ankara